

Christopher J. Melick\*, Larry L. Smith, Brian P. Pettegrew, and Patrick S. Market

*Department of Soil, Environmental, and Atmospheric Science*  
University of Missouri-Columbia  
Columbia, MO

## 1. INTRODUCTION

Curran and Pearson (1971) were among the first to investigate the regular occurrence of snow with thunder across the United States. Their study along with others (e.g., Holle and Cortinas 1998; Market et al. 2002) indicated a tendency for such events to occur over specific geographical regions, the central United States repeatedly being one of those preferred locations. Unlike the more easily identifiable surface influences, such as orographic and lake-effect processes (Schultz 1999), many cases of convective snowfall result from the release of elevated instability within the much larger circulation pattern of extratropical cyclones (ETC) (Market et al. 2002; Market et al. 2004). In particular, proximity soundings from a 30-year climatology (1961-90) performed by Market et al. (2004) reveal evidence that elevated conditional (convective) instability (CI) generally occurs with thundersnow events developing northwest of an ETC center. On the other hand, conditional symmetric instability (CSI) is usually found in northeast cases, in which the characteristic slantwise circulation pattern is oriented along baroclinic zones (i.e., banded frontal convection).

The work presented here examines the stability characteristics of thundersnow events immediately prior to initiation. In order to accomplish this objective for the winter months of 2003-04 (October-April), calculations of a growth rate parameter ( $\sigma^2$ ) from numerical weather model output will be utilized to evaluate the potential for mesoscale precipitation banding (Bennetts and Sharp 1982). Furthermore, this prognostic will aid in identifying whether the disturbance will grow or decay in the given wintertime environments, with a term by term diagnosis illustrating the type of instability present in one of the more pronounced case studies of elevated convection.

## 2. THE GROWTH RATE PARAMETER

Narrow lines of clouds and precipitation are often found in the vicinity of frontal systems. In order to explain the origin of these banded features, Bennetts and Hoskins (1979) revealed evidence through numerical modeling and observations that CSI might be an important mechanism. In their work on growth rates of slantwise convection, they obtained a doubling time for CSI on the order of a couple of hours. Subsequently, Bennetts and Sharp (1982) directly applied the relevance of CSI to the prediction of frontal rainbands by utilizing  $\sigma^2$  for small amplitude disturbances:

$$\sigma^2 = -f\zeta - \frac{RT}{p\theta_o} \frac{(\nabla_h \theta \bullet \nabla_h \theta_w)}{\frac{\partial \theta_w}{\partial p}}, \quad (1)$$

**(A)** **(B)**

in which  $\theta_o$  is a reference potential temperature (283 K),  $\theta_w$  is the wet bulb potential temperature, and the remaining variables take on their usual meteorological meanings. Units for  $\sigma^2$  are in terms of  $\text{h}^{-2}$ , with positive (negative) values expected to indicate growth (decay) of the instability. Bennetts and Sharp (1982) found that the growth rate parameter was more useful in the prediction of banded precipitation than in identifying occasions where the rainfall was uniform. In particular, the structure of any frontal precipitation was considered to be almost certainly banded for  $\sigma^2 \geq 0.2 \text{ h}^{-2}$ .

An examination of (1) reveals that several constituents contribute to the magnitude and sign of  $\sigma^2$ . Bennetts and Sharp (1982) note that conditions favorable for the development of CSI occur in regions where the two main right-hand-side terms are of similar magnitude. However, this equation also predicts positive values for  $\sigma^2$  in atmospheres characterized by other types of instability. For instance, an inertially unstable environment exists in situations when term (A)  $> 0$  and when term (A)  $\gg$  term (B). Whereas term (A) is comprised of just an inertial contribution ( $-f\zeta$ ), term (B) can be separated into three more elements. The first of these (hereafter

---

\* **Corresponding author:** Christopher J. Melick, University of Missouri-Columbia, 302 Anheuser-Busch Natural Resources Building, Columbia, MO 65211. E-mail: [cjmzr5@mizzou.edu](mailto:cjmzr5@mizzou.edu)

referred to as term B1), given by  $\frac{RT}{p\theta_o}$ ,

thermal properties of the fluid since  $R$ ,  $p$  (700-hPa), and  $\theta_o$  are all constants. As for the second contribution (hereafter referred to as term B2),  $\nabla_h \theta \bullet \nabla_h \theta_w$  corresponds to the orientation of the moisture gradient with that of the temperature gradient. The dot product stipulates that a positive (negative) sign for this particular contribution can only be obtained when the gradients point in the same (opposite) direction, such as when relatively warm air is coincident with moist (dry) air. The last of the elements (hereafter referred to as term B3) represents the moist static stability of the environment ( $\frac{\partial \theta_w}{\partial p}$ ) and generally plays a significant role

in  $\sigma^2$  as the atmosphere becomes more convectively unstable ( $\frac{\partial \theta_w}{\partial p} \rightarrow 0$ ). Therefore, as Bennetts and Sharp

(1982) emphasize, it is necessary to analyze each of the constituent parts in (1) in order to properly distinguish the type of instability present.

### 3. METHODOLOGY

METAR and SPECI observations from surface weather stations across the United States were scanned routinely during the winter months of 2003-04 (October-April). In order to document the occurrence of thundersnow during this time period, reports of thunder with various intensities of snowfall are counted. From this dataset, only events associated with an extratropical cyclone (ETC) occurring in a region roughly spanning between the Rocky and Appalachian Mountain ranges (i.e., central part of the country) were investigated further. Following the methodology applied in Market et al. (2002), fourteen separate case studies with corresponding initiation sites were subsequently identified. In order to further substantiate the true existence of thundersnow in these case studies, cloud-to-ground lightning strikes were obtained from the National Lightning Detection Network (NLDN). While oftentimes intracloud lightning will result from cold season, elevated convection, Smith et al. (2005) utilized the NLDN as a means to provide additional, solid evidence that electrical activity occurred within half of the archived snowstorms. By applying this evaluation scheme to the current work, results from this examination will be specifically restricted to the seven selected thundersnow cases given in Table I, the same subset examined in Smith et al. (2005).

Each of the right-hand-side terms in (1) were calculated, with the initial analysis from a thinned 40-km Rapid Update Cycle (RUC-2) model grid providing the necessary input data. The RUC-2 numerical weather model (Benjamin et al. 1998) is unique in its frequent hourly assimilation of the most recent observations, thus providing valuable short-range forecasts and ensuring

Table I. Information on subset of convective snow case studies examined. Location of thundersnow onset is given along with surface weather station identifier when possible. Onset time indicates year, month, date, and closest hour for which the first report occurred. The location of event with respect to associated ETC center (bearing from cyclone center) is also recorded at initiation.

TSSN Onset Location	Onset Time	Location
Salina, KS (KSLN)	0400 UTC 11-23-2003	NE
Beatrice, NE (KBIE)	1500 UTC 12-09-2003	NNE
Tulsa, OK (KRVS)	0400 UTC 12-10-2003	SW
Marion, IL (KMWA)	0400 UTC 01-27-2004	SW
Mountain Home, AR (KBPK)	0300 UTC 02-05-2004	E to NE
Near Eau Claire, WI (44.6N;90.9W)	0700 UTC 03-05-2004	NE
Hutchinson, MN (KHCD)	1300 UTC 03-13-2004	SE

better confidence when monitoring current conditions. This advantage is important in examining and noting short-term trends in stability characteristics of thundersnow events, especially considering that such phenomena have horizontal dimensions in the meso- $\beta$  scale range and typically exhibit a timescale on the order of just a few hours (e.g., Emanuel 1986; Market et al. 2002). In order to remain consistent with Bennetts and Sharp (1982), calculations of  $\sigma^2$  were performed at 700-hPa and considered significant only in regions where the relative humidity exceeded 80%. This latter criterion was applied to insure sufficient saturation of the atmosphere, a necessary condition in diagnosing the presence of CI or CSI. Finally, the validity of  $\sigma^2$  in predicting banded snowfall is assessed against observational evidence. For this purpose, the Next Generation Radar (NEXRAD) level II radar data was obtained for the time periods encompassing each case study via the National Climatic Data Center (NCDC) website: <http://has.ncdc.noaa.gov/>. The WSR-88D Algorithm Testing And Display System (WATADS) was then utilized to process and graphically display composite reflectivity patterns.

## 4. RESULTS

### 4.1 General Results from 2003-04 Winter Season

Reflectivity patterns were examined from WSR-88D radar stations in each thundersnow event except for the second to last case study, in which no suitably close radar data were available. Table II provides a diagnosis of mesoscale banding from the observational evidence, and also presents corresponding results for  $\sigma^2$ . An objective method for determining single-banded snowfall is pursued as specified by Novak et al. (2002). The

classification scheme from this particular study requires that the linear structure within the reflectivity pattern be greater than 250km in length, a width dimension of approximately 20 to 100 km, with an intensity of more than 30 dBZ maintained for longer than two hours.

An initial inspection of the stability tendencies from  $\sigma^2$  reveals considerable variations in both sign and magnitude from one episode to another (Table II). Moreover, growth of small amplitude disturbances was generally more favorable at the time that thundersnow initiated and typically verified well with the observations. In particular, the progression and sometimes intensification of already robust radar reflectivity returns (usually > 40 dBZ) into the area of interest corroborated the prediction that wintertime convection might transpire in the near future. This increase in instability is further supported by the upward trend in the average value for  $\sigma^2$  when comparing the time the event commenced ( $0.17 \text{ h}^{-2}$ ) to that from three hours prior ( $-0.45 \text{ h}^{-2}$ ). This former value corresponds to a  $\sigma$  equal to  $0.41 \text{ h}^{-1}$  or a doubling time for the disturbance every 2.4 hours, which is consistent with the established criterion ( $f^{-1}$ ) for moist slantwise convection generated from the release of CSI (e.g., Bennetts and Hoskins 1979; Emanuel 1986).

Yet, the methodology utilized by Novak et al. (2002) was too stringent for the limited number of thundersnow case studies examined in this work. Even so, banded structures appeared and persisted long enough to warrant treatment as such. Evaluation was made of these specific events by applying a simple, subjective approach. Successful forecasts in this regard applied best to the earliest (KSLN, 0400 UTC 23 November 2003) and latest (KHCD, 1300 UTC 13 March 2004) occurring case studies during the 2003-04 winter season, with the associated computed values for  $\sigma^2$  easily surpassing the  $0.2 \text{ h}^{-2}$  criterion (Table II).

#### 4.2 Case Study Analysis (13 March 2004)

The surface analysis in Fig. 1 shows a well developed cyclone positioned along the United States/Canadian border by 1300 UTC 13 March 2004. Meanwhile, another storm system was developing slightly farther to the south at the triple point in the Dakotas. Ahead of the associated warm front, a narrow line of intense precipitation stretched from north to south across southern Minnesota into central Iowa. The traditional METAR observation from Hutchinson, MN (KHCD) indicated the first occurrence of thundersnow. The existence of electrical activity in near-freezing temperatures appeared to be further substantiated with several lightning strikes from the NLDN occurring near this time around the surface station (Fig. 2). However, the elevated warm layer from the RUC-2 sounding and lack of nearby snowfall totals (not shown) suggests that some of the falling snow must have melted, possibly resulting in mixed precipitation.

Table II. WSR-88D radar stations utilized to examine each case study. The existence of mesoscale snowband(s) near time of initiation is determined from the methodology described in the text. The corresponding value for the 700-hPa growth rate parameter ( $\sigma^2$ ;  $\text{h}^{-2}$ ) is also given for three hours prior to and at thundersnow initiation for comparison against the observational evidence.

Case Study	WSR-88D	Observations	$\sigma^2$ Prior	$\sigma^2$ Onset
KSLN	TWX(Topeka, KS)	Banding	0.013	0.501
KBIE	OAX(Omaha, NE)	Cellular	0.023	0.043
KRVS	INX(Tulsa, OK)	Small Bands	-3.344	-0.17
KMWA	PAH(Paducah, KY)	Cellular	-0.11	-0.112
KBPK	SGF(Springfield, MO)	Cellular	0.03	-0.003
KHCD	MPX(Minn., MN)	Banding	0.125	0.92

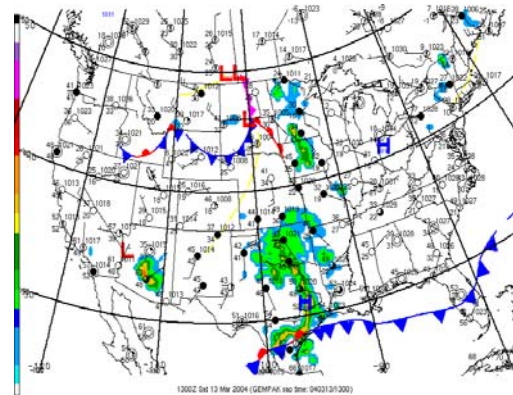


Figure 1. Surface analysis and radar reflectivity composite valid at 1300 UTC 13 March 2004. This image was obtained from: [http://www.pals.iastate.edu/archivewx/data/2004\\_03\\_13/sfc04031313.gif](http://www.pals.iastate.edu/archivewx/data/2004_03_13/sfc04031313.gif)

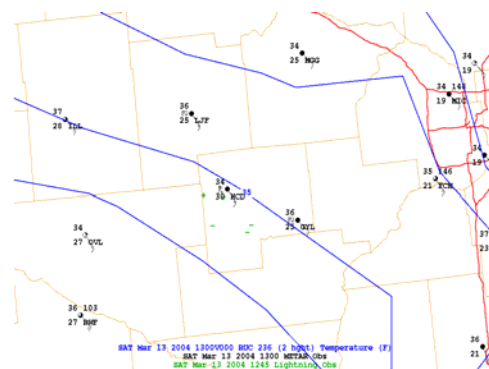


Figure 2. The 40-km RUC analysis of 2-m temperature ( $^{\circ}\text{F}$ ) and standard plotted METAR observations valid at 1300 UTC 13 March 2004. The National Lightning Detection Network (NLDN) analysis of cloud-to-ground lightning strikes valid at 1245 UTC 13 March 2004.

A more detailed analysis of the observed banding in this case study was made possible by utilizing the single WSR-88D radar reflectivity plot from Minneapolis, MN (Figure 3). This perspective revealed the previously mentioned linear feature with dimensions across the precipitation pattern appearing to be at least an order of magnitude smaller than those along the band. In addition, several intense cells were embedded throughout the system, the most impressive one residing southwest of KHCD by 1245 UTC. More specifically, intensities greater than 50 dBZ strongly indicated the presence of convective activity in the region, this justified by the cloud-to-ground lightning strikes and surface observations noted earlier (Figure 2). In order to obtain a more complete 3-D picture of the precipitation structure, however, a vertical cross-section is also taken across the reflectivity pattern of this storm. From this perspective, Figure 4 also indicates an extremely concentrated region of very high reflectivity values extending upward almost 20 kft. Thus, this tends to provide additional evidence to support the claim of banding established in the plan view evaluation.

Instability for the development of wintertime thunderstorms in southern Minnesota was also predicted rather well by noting the values and trends in  $\sigma^2$ . The RUC-2 plan view analyses shows a constricted region of positive values three hours immediately prior to the event (not shown) and at initiation (Figure 5) progressing from west to east right over the area of interest. In fact, magnitudes greater than  $0.2 \text{ h}^{-2}$  generally matched the shape and position of the banding present in the precipitation pattern (compare Figures 1, 3 with Figure 5). This latter finding is consistent with that obtained by Bennetts and Sharp (1982) and suggests that plots of  $\sigma^2$  might be beneficial to forecasters. This technique could be implemented in an operational environment and possibly provide more accurate predictions of intense rainfall or snowfall in nowcasting situations.

Determining the exact nature of the instability is permitted by partitioning the expression given in (1) into four right-hand-side terms. Upon applying this procedure, results indicate that  $\sigma^2$  is maximized at KHCD around 1300 UTC due to the combined favorable influences of terms (B1), (B2), and (B3) sufficiently offsetting the opposition from the inertial term (A). In the case of the latter, a small, negative response ( $-3.1 \times 10^{-9} \text{ s}^{-2}$ ) implies a weakly stable environment with respect to horizontal displacements. Consequently, the slightly cyclonic flow present across southern Minnesota in Fig. 6 is to be expected. Characteristic of this circulation pattern, the 700-hPa inflection axis is positioned just downstream of KHCD as an upper-level trough approaches from the west (Figure 6). Since term (B1) is always positive ( $4 \times 10^{-3} \text{ m}^3 \text{ kg}^{-1} \text{ K}^{-1}$ ) and strictly limited to fluctuations in the magnitude of the temperature (K), the

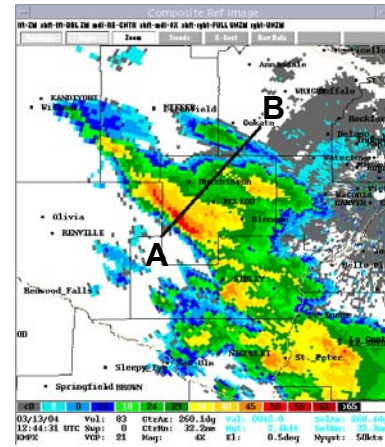


Figure 3. The radar reflectivity pattern ( $0.5^\circ$  tilt) displayed at 1245 UTC 13 March 2004 from the WSR-88D MPX radar site. Thick black line indicates cross-section across most intense part of precipitation band, as seen in Fig. 4.

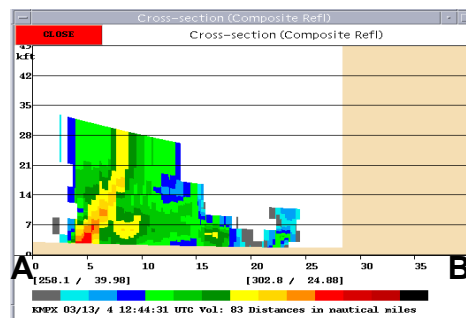


Figure 4. The radar vertical cross-section taken across most intense part of precipitation band near Hutchinson, MN from 1245 UTC 13 March 2004. Note the strongest cell and its associated tilt in the reflectivity pattern towards the northeast.

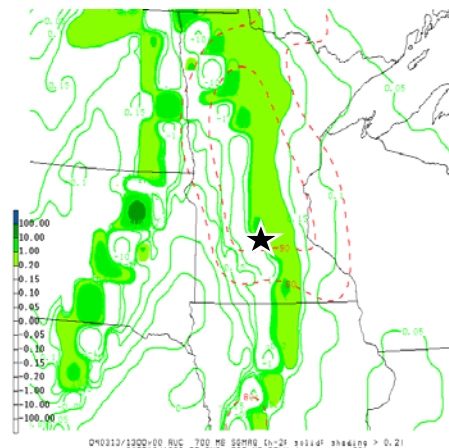


Figure 5. The 40-km RUC initial analysis of 700-hPa growth rate parameter ( $\sigma^2$ ; solid,  $\text{h}^{-2}$ ) and 700-hPa relative humidity (dashed  $> 80\%$ ) valid at 1300 UTC 13 March 2004. Green shading is applied to values of  $\sigma^2$  exceeding  $0.2 \text{ h}^{-2}$ . Star indicates approximate location of Hutchinson, MN.

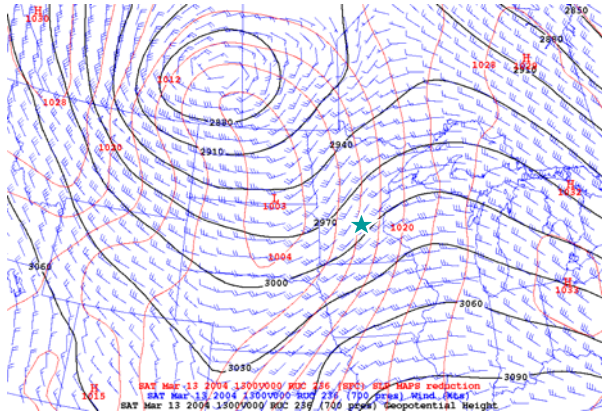


Figure 6. As in Fig. 5 except for 40-km RUC sea level pressure (solid red, hPa), 700-hPa geopotential height (solid black, gpm), and 700-hPa wind barbs (knots).

other two contributions determine the overall sign for term (B). An evaluation of the moist static stability expression (term B3) requires noting the implicit decrease in pressure with height present in the denominator. By taking this into consideration, a value of  $-1.9 \times 10^{-5} \text{ K m}^2 \text{ kg}^{-1}$  would then also indicate an atmosphere without elevated positive buoyancy present. In order to insure the desired effect on  $\sigma^2$ , the other contribution (term B2) must produce positive results, something which does occur in this case study ( $3.1 \times 10^{-10} \text{ K}^2 \text{ m}^{-2}$ ). In fact, Figure 7 showed a relatively warm, moist air mass coincident with conditions of convective stability over a large portion of eastern Minnesota, with more of a moist neutral situation influencing the KHCD vicinity. As a result, this unique assessment has eliminated the possibility of two types of instability and has left the source of the wintertime convection and associated frontal precipitation banding specifically related to the release of CSI.

Further confirmation of the stability regime can be obtained by employing other techniques. For the usual  $M_g$ - $\theta_e$  relationship, as described in Snook (1992) and Schultz and Schumacher (1999), a saturated parcel would experience an unstable slantwise path, tilted back toward the colder air, if the displacement is between the geostrophic pseudo-angular momentum ( $M_g$ ) and equivalent potential temperature ( $\theta_e$ ) surfaces. Following Moore and Lambert (1993), a vertical cross-section is constructed by first identifying the orientation of the baroclinic zone from the 850-300hPa thickness field (not shown). Endpoints for the cross-section are subsequently taken across the midtropospheric frontal zone, positioned from southwest to northeast in southern Minnesota, such that the area of interest (Hutchinson, MN) is approximately the midpoint. As a result, values of  $M_g$ ,  $\theta_e$ , and relative humidity greater than 70 % are plotted in

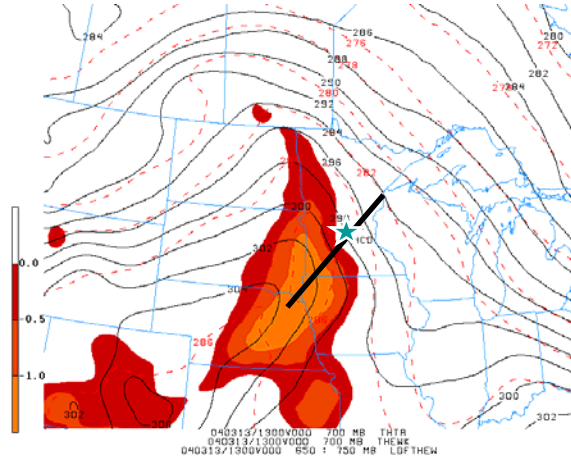


Figure 7. As in Fig. 5 except for 40-km RUC 700-hPa potential temperature ( $\theta$ ; solid, K), 700-hPa wet bulb potential temperature ( $\theta_w$ ; dashed, K), and 650-750-hPa layer difference wet bulb potential temperature (color filled < 0, K). Bold line denotes cross section line in Figs. 8 and 9.

Figure 8 on an x-z plane extending from Cloquet, MN (KCOQ) to Norfolk, NE (KOFK).

Variations in the across-frontal moist static stability are evident above the boundary layer in the vertical cross-section, with more convectively unstable conditions prevalent towards the south (Figure 8). The vertical wind shear is more pronounced, however, proceeding in the direction of the cold air with  $M_g$  surfaces at more of an inclined angle. As a result, conditions of CSI are suspected above KHCD in a shallow layer centered on 700hPa (Figure 8). In this region, slantwise accelerations are probable given that the environment is nearly saturated with relative humidity near 100 % and  $\theta_e$  surfaces steeper than  $M_g$  surfaces. Figure 9 also reveals forcing from frontogenesis collocated in the lower to middle troposphere sufficient to lift the parcels and release the instability. This inferred moist, slantwise convection is supported by an examination of the generated, ageostrophic circulation and vertical cross-section of the radar reflectivity pattern. A slightly tilted pattern in the direction of the colder air is noted in Figures 4 and 9, with relatively strong upward vertical velocities ( $8\text{-}10 \mu\text{bars sec}^{-1}$ ) restricted to mainly southern Minnesota and over the area of thundersnow.

## 5. SUMMARY AND CONCLUSIONS

Stability characteristics of thundersnow events across the central United States were studied utilizing computations of  $\sigma^2$  from RUC-2 numerical weather model output. Results were compiled for seven case studies during the 2003-04 winter season (October-April) and provided a means to confirm the likely development

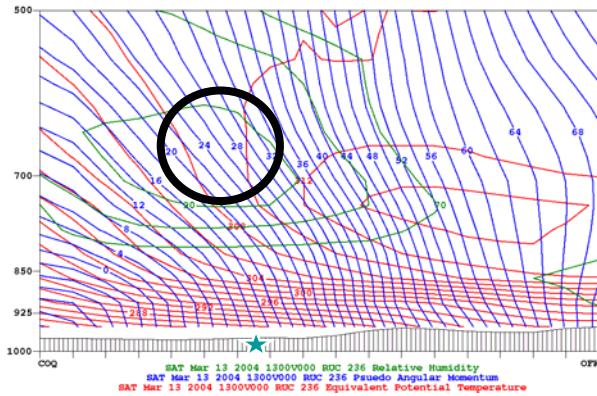


Figure 8. 40-km RUC cross-section analysis of geostrophic pseudo-angular momentum ( $M_g$ ; blue solid line,  $m s^{-1}$ ), equivalent potential temperature ( $\theta_e$ ; red solid line, K), and relative humidity greater than 70% (green solid line) valid at 1300 UTC 13 March 2004. The cross-section extends from Cloquet, MN (KCOQ) to Norfolk, NE (KOFK) with temperatures increasing to the right and the star representing approximate location of Hutchinson, MN. Solid black circle highlights atmospheric region deemed susceptible to the release of CSI.

of elevated convection. Upon comparing against observational data (e.g., METARs, NLDN, radar reflectivity), this stability tendency correctly identified that the environment was becoming destabilized immediately leading up to initiation. In particular, an upward trend in the average value of  $\sigma^2$  was obtained when comparing the time the thundersnow event commenced ( $0.17 h^{-2}$ ) to that from three hours prior ( $-0.45 h^{-2}$ ). Furthermore, this previous result corresponded to a doubling time for the convection upon the order of 2.4 hours, which was consistent with the typical timescale for moist slantwise convection generated from the release of CSI (Bennetts and Hoskins 1979; Emanuel 1986; Market et al. 2002). Finally,  $\sigma^2$  appeared to be successful in predicting the development of mesoscale precipitation banding in two of the archived case studies, similar to the findings reached by Bennetts and Sharp (1982). Verification was provided through a more realistic, subjective evaluation of the radar reflectivity data compared to the more rigid, unbiased methodology followed by Novak et al. (2002).

An in-depth analysis of one case study of significant elevated, cold-season convection (KHCD, 1300 UTC 13 March 2004) was also offered. Given the fact that  $\sigma^2$  correctly identified electrical activity within a narrow line of intense precipitation (sometimes over 50 dBZ), a term by term diagnosis of the expression was deemed feasible and necessary to properly distinguish the type of instability present. Two of the four contributions to  $\sigma^2$ , terms (A) and (B3), produced small negative responses. This tended to indicate that the atmosphere was both weakly stable to both inertial and convective influences on an air parcel. These conditions are typically found north of a warm front, such as in this particular

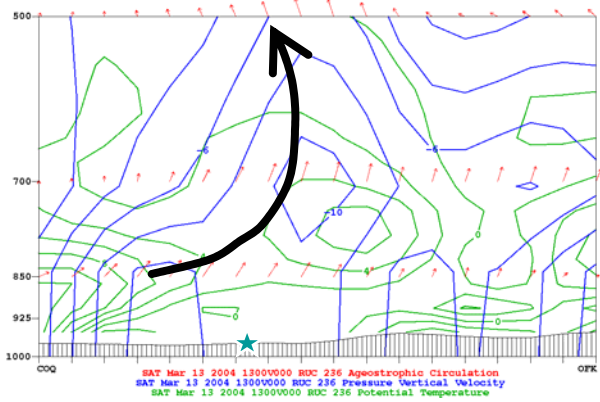


Figure 9. As in Fig. 8 except for ageostrophic circulation (vectors), isobaric vertical velocity ( $\mu\text{bars sec}^{-1}$ , blue solid lines), and 2D geostrophic frontogenesis (green solid lines,  $K 100 km^{-1} 3 hr^{-1}$ ).

event. As would be expected, the synoptic analysis revealed that the upper-level inflection axis was just downstream of a slightly cyclonic flow present in southern Minnesota, with small but positive moist static stability also evident. In a nearly saturated environment, previous work (e.g., Bennetts and Hoskins 1979; Bennetts and Sharp 1982; Bluestein 1986) has shown that this would be a preferred region for tilted convective updrafts associated with the release of CSI. Further substantiation for the assertion that CSI was present is achieved by considering the assessment from the traditional  $M_g$ - $\theta_e$  relationship. More importantly, however, the term by term diagnosis of  $\sigma^2$  also reached the same conclusion by the simple process of elimination of other types of instability.

It is hoped that some of the conclusions established by this work could be useful for routine implementation in an operational environment. Since episodes of convective snowfall often produce intense rates of precipitation over a concise time period and small spatial scale, which can often result in hazardous traveling conditions, more precise and accurate means of anticipating significant wintertime weather events are always needed by forecasters. Similar to what was recommended by Bennetts and Sharp (1982),  $\sigma^2$  could be computed easily using simple scripts with output generated from fine resolution models. This would hopefully provide another tool to help forecasters in predicting the likelihood of banded precipitation and determining the type of instability present.

**Acknowledgements** This work is supported in part by the National Science Foundation (NSF), Award No. ATM-0239010. Any opinions, findings, conclusions or recommendations expressed herein are those of the author(s) and do not necessarily reflect the views of NSF.

## REFERENCES

- Benjamin, S.G., J.M. Brown, K.J. Brundage, B.E. Schwartz, T.G. Smirnova, T.L. Smith and L.L. Morone, 1998: RUC-2 – The Rapid Update Cycle Version 2. NWS Technical Procedures Bulletin No. 448. NOAA/NWS, 18 pp. [Available online at: <http://205.156.54.206/om/tpb/448.htm>].
- Bennetts, D.A., and B.J. Hoskins, 1979: Conditional symmetric instability – a possible explanation for frontal rainbands. *Quart. J. Roy. Meteor. Soc.*, **105**, 945-962.
- \_\_\_\_\_, and J.C. Sharp, 1982: The relevance of conditional symmetric instability to the prediction of mesoscale frontal rainbands. *Quart. J. Roy. Meteor. Soc.*, **108**, 595-602.
- Bluestein, H., 1986: Fronts and jet streaks: A theoretical perspective. *Mesoscale Meteorology and Forecasting*, P.S. Ray, Ed., Amer. Meteor. Soc., 173-215.
- Curran, J.T., and A.D. Pearson, 1971: Proximity soundings for thunderstorms with snow. Preprints, *7<sup>th</sup> Conf. on Severe Local Storms*, Kansas City, MO, Amer. Meteor. Soc., 118-119.
- Emanuel, K.A., 1986: Overview and definition of mesoscale meteorology. *Mesoscale Meteorology and Forecasting*, P.S. Ray, Ed., Amer. Meteor. Soc., 1-17.
- Holle, R.L., and J.V. Cortinas, 1998: Thunderstorms observed at surface temperatures near and below freezing across North America. Preprints, *19<sup>th</sup> Conf. on Severe Local Storms*, Minneapolis, MN, Amer. Meteor. Soc., 705-708.
- Market, P.M., C.E. Halcomb, and R.L. Ebert, 2002: A climatology of thundersnow events over the contiguous United States. *Wea. Forecasting*, **17**, 1290-1295.
- \_\_\_\_\_, A.M. Oravetz, D. Gaede, E. Bookbinder, B. Pettegrew, and R. Thomas, 2004: Proximity sounding composites of midwestern thundersnow events. Preprints, *20<sup>th</sup> Conf. on Weather Analysis and Forecasting*, Seattle, WA, Amer. Meteor. Soc., CD-ROM, P4.2.
- Moore, J.T., and T.E. Lambert, 1993: The use of equivalent potential vorticity to diagnose regions of conditional symmetric instability. *Wea. Forecasting*, **8**, 301-308.
- Novak, D.R., L.F. Bosart, and D. Keyser, 2002: A climatological and composite study of cold season banded precipitation in the northeast United States. Preprints, *19<sup>th</sup> Conf. on Weather Analysis and Forecasting*, San Antonio, TX, Amer. Meteor. Soc., CD-ROM, 6.5.
- Schultz, D.M., 1999: Lake-effect snowstorms in northern Utah and western New York with and without lightning. *Wea. Forecasting*, **14**, 1023-1031.
- \_\_\_\_\_, and P.N. Schumacher, 1999: The use and misuse of conditional symmetric instability. *Mon. Wea. Rev.* **127**, 2709-2732.
- Smith, L.L., C.J. Melick, and P.S. Market, 2005: Examination of thundersnow cases in the United States utilizing NLDN data. Preprints, *Conf. on Meteorological Applications of Lightning Data*, San Diego, CA, Amer. Meteor. Soc., CD-ROM, P2.13.
- Snook, J.S., 1992: Current techniques for real-time evaluation of conditional symmetric instability. *Wea. Forecasting*, **7**, 430-439.